Scientific Research Publishing

Open Journal of Radiology, 2026, 16(3), 143-154
https://www.scirp.org/journal/ojrad
ISSN Online: 2164-3032
ISSN Print: 2164-3024

Gadolinium Enhancement Ratio in Sellar Region Masses: A Pilot Study of 16 Cases

Bénédicte Souho[1*], Géraud Akpo[2], Salif Djigo[1], Acyl Idriss[3], Pihou Gbande[4], Bidamin N'Timon[5], Abdoulatif Amadou[6], Mazamaesso Tchaou[7], Boucar Ndong[1,2], Lantam Sonhaye[3], Lama Kegdigoma Agoda-Koussema[4], Komlanvi Adjenou[3]

[1]Biophysics and Nuclear Medicine Department, Cheikh Anta Diop University, Dakar, Senegal
[2]Radiology Department, Dalal Jamm Hospital, Dakar, Senegal
[3]Radiology Department, University Teaching Hospital Campus of Lome, Lome, Togo
[4]Radiology Department, University Teaching Hospital Sylvanus Olympio, Lome, Togo
[5]Radiology Department, University Teaching Hospital in Kara, Kara, Togo
[6]Radiology Department, Tomde Regional Hospital Center, Kara, Togo
[7]Radiology Department, Lome Commune Regional Hospital Center, Lome, Togo
Email: *benesouho@yahoo.com

How to cite this paper: Souho, B., Akpo, G., Djigo, S., Idriss, A., Gbande, P., N'Timon, B., Amadou, A., Tchaou, M., Ndong, B., Sonhaye, L., Agoda-Koussema, L.K. and Adjenou, K. (2026) Gadolinium Enhancement Ratio in Sellar Region Masses: A Pilot Study of 16 Cases. *Open Journal of Radiology*, **16**, 143-154.
https://doi.org/10.4236/ojrad.2026.163015

Received: August 12, 2026
Accepted: September 21, 2026
Published: September 24, 2026

Abstract

Background: Gadolinium-based contrast agents are paramagnetic and shorten protons' T1 relaxation time. Quantitative data on T1 signal changes in sellar masses ≥ 1 cm, at 1.5T MRI, are limited. **Objective:** To quantitatively assess the paramagnetic effect of gadolinium chelate on T1 signal intensity in sellar and suprasellar masses ≥ 1 cm using 1.5T MRI, and to describe enhancement patterns according to histological type in a pilot cohort. **Methods:** Retrospective cross-sectional study of 16 patients with histologically confirmed sellar/suprasellar masses ≥ 1 cm on 1.5T MRI, between April 2021 and April 2025. Signal intensity was measured before and 4 minutes after 0.1 mmol/kg gadoteric acid injection. ROIs were placed on the solid enhancing portion of the lesion and reference white matter for pre-injection signal intensity (SIpre) and enhancement ratio (ER, expressed as percentage) calculation. **Results:** The cohort included 11 macroadenomas (68.75%), 3 craniopharyngiomas (18.75%) and 2 meningiomas (12.5%). On pre-contrast T1, 87.5% of the lesions were isointense. After gadolinium administration, all lesions showed paramagnetic enhancement. Mean ER was 30.9% ± 5.1% for macroadenomas, 53.4% ± 11.5% for craniopharyngiomas, and 89.2% ± 18.5% for meningiomas. The difference between groups was statistically significant (p = 0.0066, Kruskal-Wallis test). **Conclusion:** Quantitative analysis of MRI enhancement showed distinct profiles: intense for meningiomas, low for pituitary adenomas, and low and moderate for craniopharyngiomas. These preliminary findings suggest that enhancement ra-

tios may add to the characterization of sellar masses and should be confirmed in larger series.

Keywords

MRI, Gadolinium, Enhancement Ratio, Macroadenoma, Craniopharyngioma, Meningioma

1. Introduction

Gadolinium-based contrast agents are paramagnetic compounds widely used in magnetic resonance imaging to improve tissue contrast. Gadolinium ion Gd^{3+}, atomic number Z = 64 and molar mass M = 157.25 g/mol, is an element of the lanthanide family which possesses 7 unpaired electrons, giving it a high magnetic moment of 7.94 Bohr magnetons [1]. In MRI, gadolinium is not visualized directly. It is its effects on the surrounding protons that are observed. Through dipole-dipole interactions with adjacent water protons, Gd^{3+} shortens longitudinal relaxation time T1, resulting in increased signal intensity on T1-weighted images. This paramagnetic T1-shortening effect is the physical basis of gadolinium enhancement in MRI, observed at low concentrations of gadolinium [2].

In the intact central nervous system, gadolinium chelates do not cross the healthy blood-brain barrier (BBB). However, the sellar and suprasellar regions contain anatomical structures located outside the BBB, including the pituitary gland and pituitary stalk, which normally enhance homogeneously after gadolinium injection, in the absence of pathology [2] [3]. Pathological masses in this region, such as pituitary adenomas, craniopharyngiomas, and meningiomas, disrupt the local microenvironment and modify gadolinium diffusion and T1 relaxation. The resulting enhancement patterns are routinely used by radiologists for etiological diagnosis. However, most studies rely on visual assessment of enhancement intensity and homogeneity, which remains reader-dependent.

Quantitative assessment of the paramagnetic effect through signal intensity measurements and calculation of enhancement ratios provides more objective biophysical data on T1 relaxation changes induced by gadolinium. Such quantitative parameters are particularly relevant at 1.5T MRI, which remains the most widely available field strength in low-resource settings. Quantitative data on gadolinium-induced changes in sellar/suprasellar masses ≥ 1 cm are limited. Accurate pre-operative differentiation of these masses is crucial for their treatment strategies and prognoses. For example, pituitary adenomas are often managed medically or by transsphenoidal surgery while meningiomas and craniopharyngiomas frequently require craniotomy and carry different surgical risks [4].

The aim of this pilot study was to quantitatively assess the paramagnetic effect of gadolinium chelate on T1 signal parameters in sellar and suprasellar masses ≥ 1 cm, at 1.5T MRI, and to describe enhancement patterns according to histological type.

2. Methods

2.1. Study Design and Population

This retrospective cross-sectional study was conducted at the imaging department of Dalal Jamm Hospital, Dakar, Senegal, between April 2021 and April 2025.

Patients who underwent gadolinium-enhanced imaging on 1.5T MRI, with histologically confirmed sellar or suprasellar masses ≥ 1 cm, were included. Exclusion criteria were: mass < 1 cm, mass without solid component, motion artifacting ROI placement, history of prior surgery or radiotherapy and incomplete DICOM data.

A total of 96 pituitary MRIs were performed during the study period, of which 54 revealed a known or newly diagnosed sellar and/or parasellar, 36 were normal and 6 examinations were lost. Among the 54 abnormal examinations, some patients were eligible for surgery. Histological results were available for 19 of them; the other patients were lost to follow-up. Of these 19 patients, 3 did not meet the inclusion criteria due to incomplete MRI in 2 patients and a lesion < 1 cm in 1 patient, leaving 16 patients included in the final analysis.

2.2. MRI Protocol

All examinations were performed using a head coil on a 1.5T HITACHI MRI, model Echelon Smart, operational since March 2021.

Figure 1. Head of the automatic dual syringe injector (A) and its control room unit (B).

A standard protocol was applied to all patients. Pre-contrast T1-weightened high-resolution (HR) spin-echo (SE) sequences were acquired in sagittal and axial planes: TR 400 - 600 ms, TE 8 - 12 ms, slice thickness 3 - 4 mm. Dynamic contrast enhance-

ment was performed after intravenous injection of 0.1 mmol/kg gadoteric acid, at a concentration of 0.5 mmol/mL at 2 mL/s followed by 20 mL of saline flush, using an automatic double-syringe injector (**Figure 1**). Dynamic post-contrast T1-weighted images were acquired immediately after injection during 5 to 6 minutes. Other sequences, such as T2-weighted SE HR, Flair, Gradient Echo, and Diffusion, were performed, supplemented by acquisitions of the entire brain volume in 3D T1 SE and T1 SE after gadolinium injection in axial slices.

For this study, we examined only the ES 3D T1 HR sequences (TE at 8 - 20 ms and TR at 400 - 550 ms), ES 3D T1 throughout the entire brain volume for very large lesions, and dynamic T1-weighted sequences (TE at 8 - 20 ms and TR at 500 - 900 ms).

2.3. Quantitative Analysis

Signal intensity (SI) measurements were performed by one senior radiologist blinded to histology, using Myrian version 2.7.6 reading software. For each lesion, T1 signal intensity ratio and enhancement ratio were calculated.

For T1 signal intensity ratio calculation, a circular ROI was manually placed on the solid enhancing portion of the mass on pre-contrast (SI pre-lesion), avoiding cystic, necrotic or hemorrhagic areas. A reference ROI was placed on normal-appearing white matter at temporal lobe (SI pre white matter). Due to background signal suppression, noise measured in air was zero. Then, the T1 pre-injection signal intensity ratio (SIr pre) was calculated by Formula (1):

$$\text{SIr pre} = \frac{\text{SI pre lesion}}{\text{SI pre white matter}} \quad (1)$$

The mass was classified hypointense for a SIr pre < 0.8; hyperintense for SIr pre > 1.2 and isointense for the rest (**Figure 2** and **Figure 3**).

For enhancement ratio calculation, a circular ROI of 10 - 25 mm^2 was manually placed on the solid enhancing portion of the mass, avoiding cystic, necrotic or hemorrhagic areas, on dynamic T1 images, at 0 minutes corresponding to the start of injection (SI pre gadolinium) and 4 minutes (SI post gadolinium). This time point was chosen to allow for contrast diffusion into interstitial space of solid tumor component while avoiding late-phase washout [5]. The ROIs were placed on the same dynamic sequence using the acquisition time displayed on the screen as a reference. A second, synchronously acquired sequence (T2 ES) was viewed in parallel to ensure that the second ROI was positioned in exactly the same location as the first. The enhancement ratio (ER) was calculated with Formula (2):

$$\text{ER} = \frac{\text{SI post gadolinium} - \text{SI pre gadolinium}}{\text{SI pre gadolinium}} \times 100 \quad (2)$$

Enhancement intensity was classified as weak for ER < 50%, intense for ER > 100% and moderate for the rest (**Figure 4**).

The injected sequences, as well as other sequences such as the T2* sequence and the T2-weighted ES sequence, were sometimes used to better distinguish between tissue and non-tissue portions.

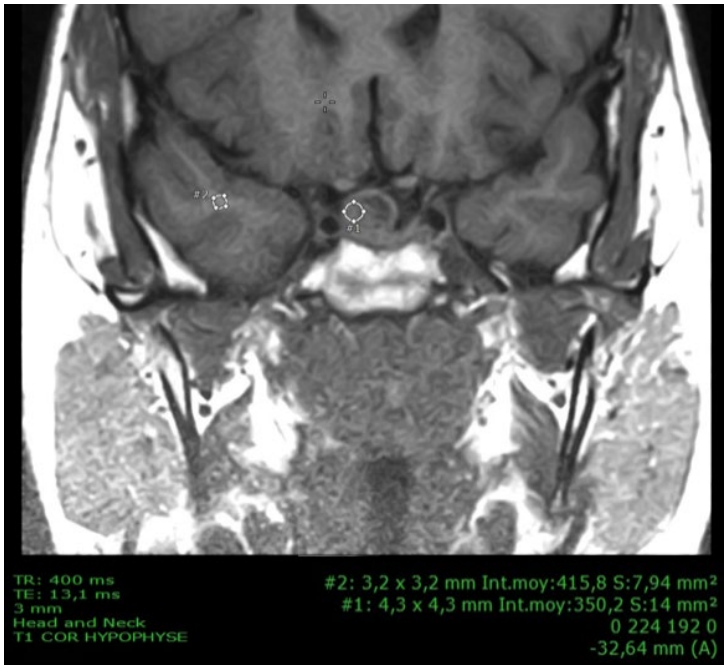

Figure 2. Sellar and suprasellar lesion on T1-weighted MRI in a 38-year-old female patient presenting with hyperprolactinemia. ROI 1 (solid portion of the lesion) = 116.9 and ROI 2 (temporal white matter) = 161.5, yielding a ROI 1/ROI 2 ratio of 0.72, consistent with a T1 hypointense lesion.

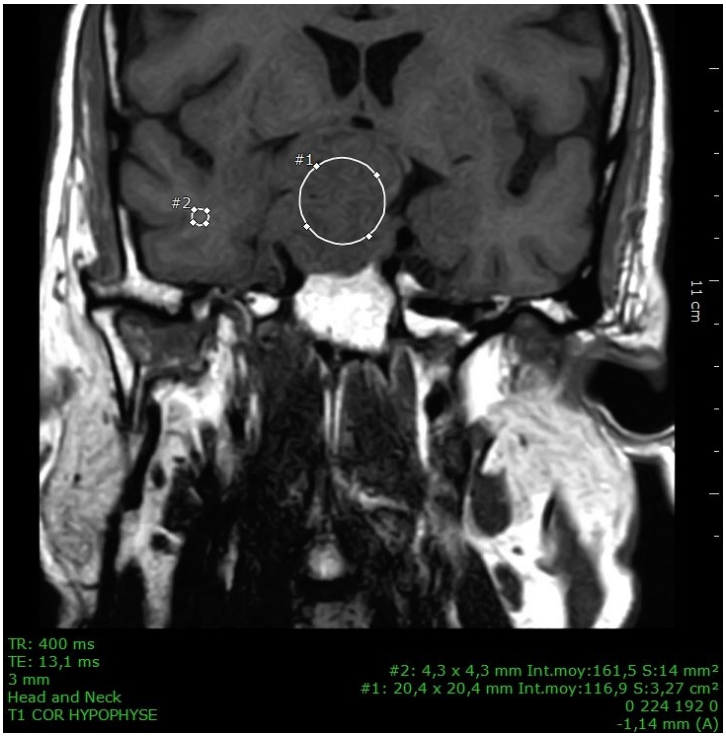

Figure 3. Sellar lesion on T1-weighted MRI in a 42-year-old male patient presenting with headache and visual disturbances. ROI 1 (solid component of the lesion) = 350.2 and ROI 2 (temporal white matter) = 415.8, yielding a ROI 1/ROI 2 ratio of 0.84, consistent with a T1 isointense lesion.

The homogeneous or heterogeneous nature of the enhancement was analyzed visually. The data were recorded in Excel 2016 software.

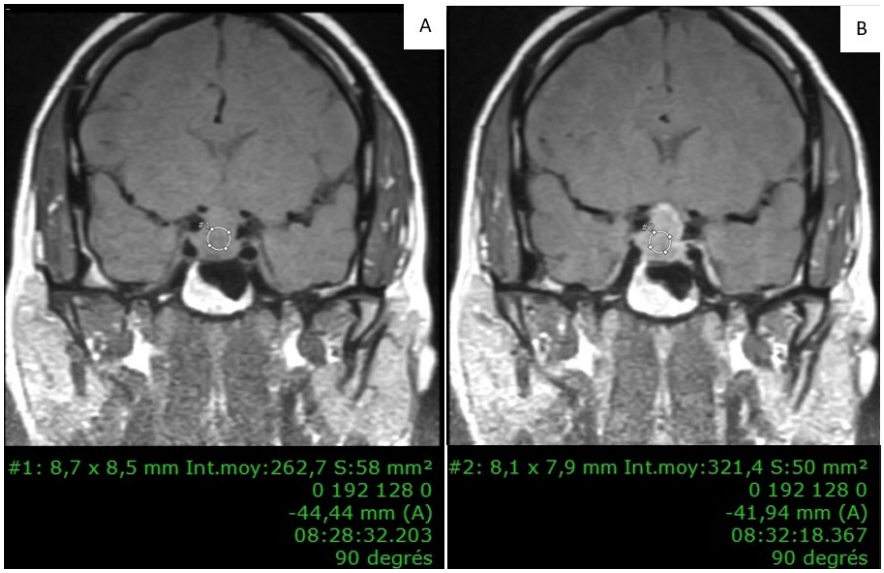

Figure 4. T1-weighted dynamic contrast-enhanced MRI with gadolinium injection, showing a sellar lesion with suprasellar extension, in a 37-year-old female patient presenting with visual disturbances and amenorrhea, showing a sellar and suprasellar mass. ROI pre-injection (SI pre) = 262.7 (A) and ROI 4 minutes after injection (SI post) = 321.4 (B). The calculated enhancement ratio is 22.34%, consistent with a weak enhancement.

2.4. Parameters Studied

The parameters studied were: age and sex of patients, histological diagnosis, lesion size, lesion location, T1 signal intensity of the solid portion (hypointense, isointense, hyperintense), gadolinium uptake assessed by its absence or presence, its intensity (low, moderate, or high) and its homogeneous or heterogeneous nature.

Quantitative variables were described by measures of central tendency (mean, median) and measures of dispersion (standard deviation, range). Qualitative variables were described using counts and percentages. Kruskal-Wallis H test was used for comparison of ER between histological groups due to small sample size and non-normal distribution. Post-hoc analysis was performed using Dunn's test with Bonferroni correction. Effect size was reported as epsilon-squared with 95% confidence intervals. A p-value < 0.05 was considered significant. The significant omnibus Kruskal-Wallis result was not interpreted as evidence of pairwise differences between specific groups.

3. Results

3.1. Age and Sex of Patients

The patients had a mean age of 44 ± 19.48 years [6 years; 79 years] and the median age was 44 years. The sex ratio was 1. The distribution of patients by age and gender is illustrated in **Figure 5**.

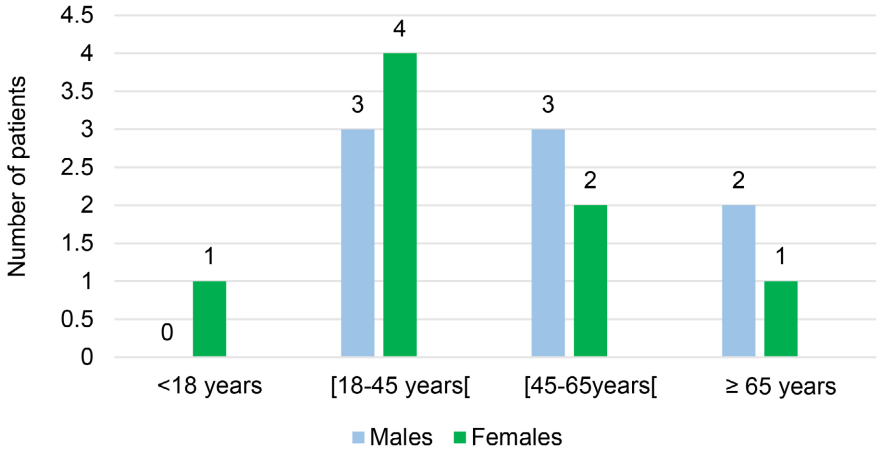

Figure 5. Distribution of patients by age group and gender.

3.2. Histology Diagnoses, Size and Location of Lesions

After histology, the diagnoses were 11 adenomas (68.75%), 3 craniopharyngiomas (18.75%) and 2 meningiomas (12.5%).

The adenomas had an average size of 32.54 ± 16.88 mm, with extremes of 12 mm and 57 mm and a median of 38 mm. They were all intrasellar with suprasellar extension.

Craniopharyngiomas had an average size of 54.40 ± 17.39 mm [34.9 mm; 68.3 mm] and a median size of 60 mm. Two craniopharyngiomas (66.67%) were strictly suprasellar and one craniopharyngioma (33.33%) was suprasellar with intrasellar extension.

The two meningiomas had an average size of 43.1 ± 6.08 mm and were located in the left laterosellar region in both cases.

3.3. T1 Pre-Injection Signal Intensity Ratio

On T1-weighted images without gadolinium injection, 14 (87.5%) of all lesions were isointense and 2 (12.50%) were hypointense.

Adenomas were isointense in 9/11 cases (81.82%) with an average Sir pre of 0.95 [0.85; 1.1] and hypointense in 2/11 cases with an average Sir pre of 0.78 (18.18%).

Craniopharyngiomas were T1 isointense in 100% of cases (3/3 cases) with an average Sir pre of 1.02 [0.94; 1.13].

Meningiomas were T1 isointense in 100% of cases (2/2 cases) with an average Sir pre of 1.05.

3.4. Intense or Moderate Gadolinium Uptake

After injection, all lesions (16 lesions, or 100%) showed signs of gadolinium uptake. Table 1 shows the ER by histology.

3.5. Homogeneous or Heterogeneous Gadolinium Enhancement

Eight adenomas (72.73%) were heterogeneous, always associated with central ne-

crotic areas with T1 hypointense (8 cases) and, in addition, hemorrhage with T1 hyperintense in 2 cases. Two craniopharyngiomas were heterogeneous, related to cystic portions and signal voids (Figure 6). Meningiomas were homogeneous.

Table 1. Enhancement ratio (ER) by histology.

Histology	n	Mean ER ± SD	Min-Max	Median
Pituitary macroadenoma	11	30.93 ± 4.89	22.8 - 39.02	31.6
Craniopharyngioma	3	53.37 ± 12.20	45.6 - 67.4	47.1
Meningioma	2	89.20 ± 18.53	76.1 - 102.3	89.2
Total	16	42.43 ± 21.16	22.8 - 102.3	33.55

Kruskal-Wallis test: p-value = 0.0066; H = 10.04; ER: enhancement ratio; SD: standard deviation.

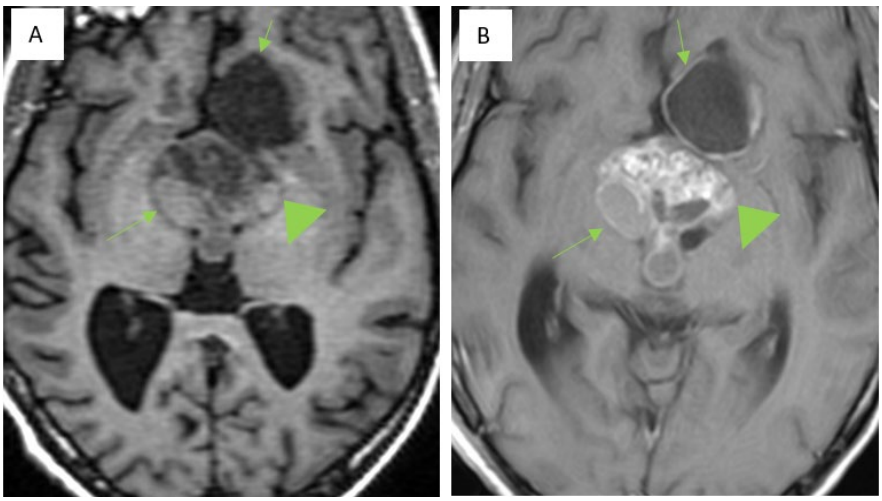

Figure 6. T1-weighted MRI before (A) and after (B) gadolinium administration in a 17-year-old male patient with growth and visual disturbances, showing a heterogeneous craniopharyngioma. The solid component shows punctate signal voids (arrowhead), and the cystic components show no enhancement (arrows).

4. Discussion

4.1. Limitations

This study has several limitations. First, although the difference in ER between groups reached statistical significance, the sample size remains small, limited to 16 patients. These results should be considered preliminary. The small number of meningiomas and craniopharyngiomas limits the reliability of effect size estimates and prevents meaningful post-hoc pairwise comparison. This reflects both the single-center, retrospective design and the relative rarity of certain sellar and suprasellar masses, particularly craniopharyngiomas and meningiomas [6]-[8]. Second, signal intensity measurements were performed manually using circular ROIs. This

approach may introduce inter- and intra-observer variability, despite standardization of ROI size and placement. Third, the single-center design using a 1.5T MRI system limits the generalizability of our findings to other field strengths [9].

Despite these limitations, this pilot study provides preliminary quantitative data on gadolinium-induced T1 signal changes in supracentimetric sellar masses imaged at 1.5T. The observed biophysical trends warrant further validation in larger, prospective, multicenter studies with standardized acquisition protocols and automated segmentation techniques.

4.2. Lesion Signal Intensity in T1

Following quantitative analysis, 87.5% of lesions were isointense on T1-weighted images. This predominance of T1 isointensity suggests that most solid sellar masses have T1 relaxation times similar to that of white matter at 1.5T. White matter is commonly used as a reference because it has stable and easily identifiable signal. Our findings are consistent with those of Diop *et al.*, who also reported a majority of T1 isointensity in these pituitary [10]. Similarly, other series have described T1 isointensity as the most common pattern of these lesions [11] [12]. In contrast, Ohui Acko *et al.* and Garba *et al.* reported predominance of T1 hypointense sellar masses [13] [14]. This difference may be related to methodological differences, as visual assessment remains subjective and operator-dependent, whereas quantitative signal measurement using ROI analysis provides more reproducible and objective data. Furthermore, differences in field strength, sequence parameters and lesion composition may also account for this variability.

From a diagnostic perspective, T1 isointensity alone is non-specific, as quantitative T1 assessment shows that isointensity is the dominant signal pattern in solid sellar lesions at 1.5T. But when combined with enhanced contrast patterns and morphological characteristics, it may help narrow the differential diagnosis of sellar masses.

4.3. Enhancement Ratio

Gadolinium-based contrast agents are paramagnetic T1 agents that shorten the longitudinal relaxation time T1 of surrounding tissues [1] [15]. The magnitude of T1 shortening depends on tissue vascularity, capillary permeability and extracellular distribution of gadolinium [16]. In our study, acquisition time was standardized and all patients received the same dose, therefore differences in ER primarily reflect intrinsic tissue properties.

Significant differences in ER were observed between histological groups ($H = 10.04$; $p = 0.0066$).

Meningiomas showed moderate enhancement but the highest mean ER (89.2% ± 18.5%). This is consistent with their rich arterial vascularization and lack of BBB, allowing free diffusion of gadolinium into the extracellular space [17].

Macroadenomas showed the lowest enhancement with a mean ER of 30.9% ± 5.1%. This weak enhancement may be related to altered vascularization, develop-

ment of an inefficient arterial blood supply and to the presence of fibrous tissue or microhemorrhages, which reduce gadolinium distribution [1] [18]. Our results are in line with studies reporting moderate to low enhancement in pituitary macroadenomas [12] [19]. In contrast, Garba *et al.* reported intense enhancement of macroadenomas based on visual assessment [14]. This discrepancy may be explained by the subjective nature of visual evaluation.

Craniopharyngiomas had inter-mediate ER values with a mean ER of 53.4% ± 11.5%. The presence of microcalcification in solid areas could lower the overall ER. This is consistent with literature describing variable enhancement patterns in craniopharyngiomas depending on their adamantinomatous or pipillary subtype [20] [21].

Thus, ER appears useful for the differential diagnosis of sellar lesions.

4.4. Homogeneous or Heterogeneous Enhancement

The pattern of enhancement reflects underlying tissue architecture and vascular distribution. Homogeneous enhancement typically occurs in lesions with uniform cellularity and vascularity, while heterogeneous enhancement results from necrosis, cystic portions, hemorrhage, or calcification.

In this study, meningiomas and some macroadenomas showed homogeneous enhancement, consistent with their compact cellular structure and uniform vascular supply. In contrast, some adenomas and craniopharyngiomas demonstrated heterogeneous enhancement. For craniopharyngiomas, this is explained by their mixed components, even though signal analysis was performed on the solid portion only [20]. Focal signal voids observed in craniopharyngiomas corresponded to calcifications. Serpiginous signal voids in meningiomas usually reflect flow voids from hypervascular vessels [22].

5. Conclusion

This pilot study suggests that quantitative assessment of post-gadolinium enhancement could help differentiate sellar region masses. Meningiomas showed moderate enhancement and the highest enhancement ratio with a mean ER of 89.20 ± 18.53. Pituitary adenomas showed low enhancement with a mean ER of 30.93 ± 4.89. For craniopharyngiomas, enhancement of the solid portion was low and moderate with a mean ER of 53.37 ± 12.20. These differences in ER may reflect variations in the vascularization of these tumors. Quantitative analysis of enhancement may provide additional data to complement morphological criteria and qualitative analysis. The main limitations were a small sample size and a retrospective design of the study. Larger prospective studies are needed to validate these enhancement thresholds and establish their diagnostic value in clinical practice.

Author Contributions

All authors contributed to the drafting, review and approval of the final version of the manuscript.

Conflicts of Interest

The authors declare no conflicts of interest regarding the publication of this paper.

References

[1] Idée, J.M., Fretellier, N., Thurnher, M.M., Bonnemain, B. and Corot, C. (2015) Physico-chimie et profil toxicologique d'agents de contraste pour l'imagerie par résonance magnétique, les chélates de gadolinium. *Annales Pharmaceutiques Françaises*, **73**, 266-276. https://doi.org/10.1016/j.pharma.2015.01.001

[2] Kastler, B. and Vetter, D. (2011) Understanding MRI: A Self-Study Guide. 7e Édition, Elsevier Masson, 407 p.

[3] Trouillas, J., Catala, M. and Girod, C. (2007) Anatomy and Histology of the Human Pituitary Gland. EMC (Elsevier Masson SAS, Paris), Endocrinologie-Nutrition, 10-017-B-10.

[4] Gaillard, S. and Aniba, K. (2010) Aspects neurochirurgicaux des adénomes hypophysaires. *EMC—Endocrinologie—Nutrition*, **21**, 1-19. https://doi.org/10.1016/s1155-1941(10)51188-0

[5] Sakamoto, Y., Takahashi, M., Korogi, Y., Bussaka, H. and Ushio, Y. (1991) Normal and Abnormal Pituitary Glands: Gadopentetate Dimeglumine-Enhanced MR Imaging. *Radiology*, **178**, 441-445. https://doi.org/10.1148/radiology.178.2.1987606

[6] Alboqami, M.N., Khalid S Albaiahy, A., Bukhari, B.H., Alkhaibary, A., Alharbi, A., Khairy, S., *et al.* (2024) Craniopharyngioma: A Comprehensive Review of the Clinical Presentation, Radiological Findings, Management, and Future Perspective. *Heliyon*, **10**, e32112. https://doi.org/10.1016/j.heliyon.2024.e32112

[7] Momin, A.A., Recinos, M.A., Cioffi, G., Patil, N., Soni, P., Almeida, J.P., *et al.* (2021) Descriptive Epidemiology of Craniopharyngiomas in the United States. *Pituitary*, **24**, 517-522. https://doi.org/10.1007/s11102-021-01127-6

[8] Glezer, A., Paraiba, D.B. and Bronstein, M.D. (2008) Rare Sellar Lesions. *Endocrinology and Metabolism Clinics of North America*, **37**, 195-211. https://doi.org/10.1016/j.ecl.2007.10.003

[9] Portocarrero-Ortiz, L., Bonifacio-Delgadillo, D., Sotomayor-González, A., Garcia-Marquez, A. and Lopez-Serna, R. (2010) A Modified Protocol Using Half-Dose Gadolinium in Dynamic 3-Tesla Magnetic Resonance Imaging for Detection of ACTH-Secreting Pituitary Tumors. *Pituitary*, **13**, 230-235. https://doi.org/10.1007/s11102-010-0222-y

[10] Diop, A.D., Ba Diop, S., Dia, A.N., *et al.* (2014) Aspects épidémiologiques et IRM des lésions de la région sellaire et parasellaire à Dakar (Sénégal). *Journal Africain d'Imagerie Medicale*, **6**, 13-22.

[11] Sushma, B., Sukumar, R. and Ramesh, V.K.V. (2024) Magnetic Resonance Evaluation of Sellar or Parasellar Masses in Correlation with Histopathology. *European Journal of Cardiovascular Medicine*, **13**, 1032-1037.

[12] Admin, A., Franck, M.R., Nestor, A., *et al.* (2021) Profil épidémiologique et aspect à l'IRM des pathologies hypophysaires au CHU de Brazzaville. *Journal Africain d'Imagerie Médicale*, **13**, 31-35. https://doi.org/10.55715/jaim.v13i1.183

[13] Ohui Acko, E.V., Kouadio, K.E., Gui-Bilé, L.N., Kabas, R.M., *et al.* (2017) IRM des pathologies sellaires et supra sellaires à Abidjan: À propos de 65 cas. *Journal Africain d'Imagerie Médicale*, **2017**, 112-117.

[14] Garba, I., Tchimou, A., Soro, Y.E. and Coulibaly, A. (2022) Aspects en imagerie par résonance magnétique des lésions sellaires et parasellaires identifiées au CHU d'An-

gré [MRI Aspects of Sellar and Parasellar Lesions Identified at CHU d'Angré]. *The Journal of the Royal Musical Association*, **1**, 112-121. https://www.revues-ufhb-ci.org/?parcours=revues&desc=5&arti=3462

[15] Ibrahim, M.A., Hazhirkarzar, B. and Dublin, A.B. (2026) Gadolinium-Based MRI Contrast Agents. StatPearls Publishing. https://www.ncbi.nlm.nih.gov/books/NBK482487/

[16] Gordon, Y., Partovi, S., Müller-Eschner, M., Amarteifio, E., *et al.* (2014) Dynamic Contrast-Enhanced Magnetic Resonance Imaging: Fundamentals and Application to the Evaluation of the Peripheral Perfusion. *Cardiovascular Diagnosis and Therapy*, **4**, 147-164.

[17] Ansari, S.F., Shah, K.J., Hassaneen, W. and Cohen-Gadol, A.A. (2020) Vascularity of Meningiomas. In: *Handbook of Clinical Neurology*, Jaypee Brothers Medical Publishers, 153-165.

[18] Yuh, W.T., Fisher, D.J., Nguyen, H.D., Tali, E.T., Gao, F., *et al.* (1994) Sequential MR Enhancement Pattern in Normal Pituitary Gland and in Pituitary Adenoma. *American Journal of Neuroradiology*, **15**, 101-108.

[19] Harzallah, L., Boudabbous, S., Migaw, H., Harzallah, F., Ach, K., Hamdi, I., *et al.* (2006) IRM et adénomes hypophysaires. *Annales d'Endocrinologie*, **67**, 325-330. https://doi.org/10.1016/s0003-4266(06)72606-3

[20] Traore, Z., Camara, O., Benouna, S., Lamrani, Y., Boubbou, M., Tizniti, S., *et al.* (2015) Imagerie des craniopharyngiomes. *Revue Neurologique*, **171**, A135. https://doi.org/10.1016/j.neurol.2015.01.317

[21] Van Effenterre, R. and Boch, A.L. (2007) Les craniopharyngiomes. *Annales d'Endocrinologie*, **68**, 412-421. https://doi.org/10.1016/j.ando.2007.08.001

[22] Wang, C., Xu, Y., Xiao, X., Zhang, J., Zhou, F. and Zhao, X. (2016) Role of Intratumoral Flow Void Signs in the Differential Diagnosis of Intracranial Solitary Fibrous Tumors and Meningiomas. *Journal of Neuroradiology*, **43**, 325-330. https://doi.org/10.1016/j.neurad.2016.06.003